Annals of Nuclear Energy 181 (2023) 109521

Contents lists available at ScienceDirect

Annals of Nuclear Energy

journal homepage: www.elsevier.com/locate/anucene

On the simulation of neutron noise induced by vibrations of fuel pins in a fuel assembly

P. Vinai [a,*], H. Yi [a], C. Demazière [a], A. Rouchon [b], A. Zoia [b], A. Vidal-Ferràndiz [c], A. Carreño [c], D. Ginestar [c], G. Verdú [c]

[a] Department of Physics, Chalmers University of Technology, SE-41296 Gothenburg, Sweden
[b] Université Paris-Saclay, CEA, Service d'Etudes des Réacteurs et de Mathématiques Appliquées, 91191, Gif-sur-Yvette, France
[c] Universitat Politècnica de València, Camino de Vera s/n, 46022 València, Spain

ARTICLE INFO

Keywords:
Reactor neutron noise modelling
Monte Carlo
Deterministic transport methods
Diffusion

ABSTRACT

Vibrations of fuel assemblies are an important issue in the safe operation of nuclear reactors, because they can challenge the integrity of the fuel with potential for radioactive releases. Reactor neutron noise-based techniques for monitoring vibrations are valuable for core diagnostic since they are not intrusive and make use of ordinary neutron flux measurements from ex-core and in-core detectors. The application of these techniques involves the solution of inverse problems that require numerical simulations capable of estimating the reactor neutron noise, given a model of the vibrations. For this purpose, several novel reactor neutron noise solvers have been developed in the CORTEX project using either Monte Carlo or deterministic methods, such as the discrete ordinates method, the method of characteristics, and the diffusion approximation. In the current work, these solvers have been scrutinized by computing the neutron noise induced by vibrations of one or multiple fuel pins in a simplified UOX fuel assembly benchmark, via proper variations of macroscopic neutron cross sections. The comparison of these neutron noise solutions obtained from the different methods shows novel insights into the simulation of neutron noise induced by mechanical vibrations, such as the challenges posed by the Monte Carlo method, the impact of the angular discretization on the application of the discrete ordinates method, and the accuracy of the diffusion approximation assessed via the higher-order neutron transport methods.

1. Introduction

In normal operation of a nuclear reactor, it is of paramount importance to monitor the instantaneous state of the core in order to identify and promptly correct perturbations that might compromise safety. Among these perturbations, vibrations of fuel assemblies in the core induced by the coolant flow or coolant boiling are of particular concern, because they can lead to failures with potential for radioactive releases, via mechanical and local overheating phenomena. A possible approach for online monitoring of vibrations in the core is based on the analysis of reactor neutron noise, i.e., the stationary, small fluctuations in the neutron flux measurements obtained from the ex-core and in-core neutron detectors, e.g., see (Park et al., 2003) and (Tran et al., 2015). Neutron noise depends on the stochastic character of the nuclear fission chain process and neutron correlations, while reactor neutron noise is associated with the neutron flux in a nuclear reactor and includes the effect of perturbations that make the reactor properties fluctuate. In the current work, only the neutron noise arising from periodic spatial oscillations of specific regions within a neutron multiplying system is considered.

For the analysis of reactor neutron noise, numerical simulations that reproduce the response of the system to the perturbations are often mandatory to solve the inverse problem, allowing the identification of the source of noise (e.g., a faulty fuel rod or fuel assembly) from a collection of measured signals. These simulations are usually based on diffusion theory because their computational cost is relatively cheap and because lower-order, coarse modelling is generally considered adequate for reactor neutron noise-based core diagnostics, e.g., see (Pázsit, 1992). However, diffusion-based approximations need to be verified and validated against, if available, experimental data and against reference solutions produced with higher-order computational neutron transport methods.

Neutron diffusion theory was used to model and calculate neutron noise induced by fuel assembly vibrations in previous research, e.g., see

* Corresponding author.
E-mail address: vinai@chalmers.se (P. Vinai).

https://doi.org/10.1016/j.anucene.2022.109521
Received 8 June 2022; Received in revised form 20 September 2022; Accepted 18 October 2022
Available online 27 October 2022

(Chionis et al., 2020), (Vidal-Ferràndiz et al., 2020a), (Verma et al., 2021), (Mylonakis et al., 2021), and (Vidal-Ferràndiz et al., 2022). These types of diffusion-based simulations with fuel assembly vibrations have never been evaluated against higher-order reference solutions. Thus, the paper presents a first-of-its-kind study in which diffusion methods are compared with higher-order transport methods via neutron noise problems with one or several fuel pins displaying mechanical vibrations in a simplified fuel assembly. The paper also gives novel insights into the challenges that must be considered when calculating reference solutions with Monte Carlo and deterministic transport methods in problems of neutron noise induced by mechanical vibrations. For the investigation, lower- and higher-order neutron noise solvers developed in the CORTEX project (Demazière et al., 2018) are used, namely the stochastic solver in the Monte Carlo code TRIPOLI-4® (Rouchon et al., 2019), the integro-differential transport lattice solver in APOLLO3® (Rouchon et al., 2020), the discrete ordinates solver NOISE-SN (Yi et al., 2021), the diffusion-based solver CORE SIM+ (Mylonakis et al., 2021), and the diffusion-based framework FEMFFUSION (Vidal-Ferràndiz et al., 2020a).

These computational tools together with the Monte Carlo algorithm from Kyoto University (Yamamoto, 2013, and Yamamoto, 2018) were already compared for the simpler case of a fluctuation imposed to the material properties of a single fuel pin in the simplified fuel assembly, see (Vinai et al., 2021). The main conclusion of this previous study was that the diffusion and transport methods may provide similar results, although discrepancies were found close to the location of the perturbation or where the material properties change abruptly.

The paper is structured as follows. In section 2, the theoretical framework for reactor neutron noise simulations and the numerical solvers used in the work are introduced. In section 3, the specifications of the simplified fuel assembly are provided and two neutron noise problems with vibration of fuel pins are defined. In section 4, the modelling of the vibrations is discussed. In sections 5, the neutron noise calculated with the different solvers in the two problems is analyzed. In section 6, conclusions are drawn.

2. Reactor neutron noise equations and solvers

In a neutron-multiplying system, the spatial distribution of the neutron population and its time evolution may be determined with the multi-energy-group time-dependent neutron transport equation together with balance equations for the delayed-neutron precursors, i.e.:

$$\left[\frac{1}{\mathrm{v_g}}\frac{\partial}{\partial \mathrm{t}}+\mathbf{\Omega}\bullet\nabla+\Sigma_{\mathrm{t,g}}(\mathbf{r},\mathrm{t})\right]\psi_{\mathrm{g}}(\mathbf{r},\mathbf{\Omega},\mathrm{t})=$$
$$\int_{4\pi}\sum_{\mathrm{g}'}\Sigma_{\mathrm{s,g}'\to\mathrm{g}}(\mathbf{r},\mathbf{\Omega}'\to\mathbf{\Omega},\mathrm{t})\psi_{\mathrm{g}'}(\mathbf{r},\mathbf{\Omega}',\mathrm{t})d\mathbf{\Omega}'$$
$$+\frac{\chi_{\mathrm{p,q}}(\mathbf{r})}{4\pi}\left(1-\sum_{\mathrm{q}}\beta_{\mathrm{q}}(\mathbf{r})\right)\sum_{\mathrm{g}'}\nu\Sigma_{\mathrm{f,g}'}(\mathbf{r},\mathrm{t})\phi_{\mathrm{g}'}(\mathbf{r},\mathrm{t})+\frac{1}{4\pi}\sum_{\mathrm{q}}\chi_{\mathrm{d,q,g}}(\mathbf{r})\lambda_{\mathrm{q}}C_{\mathrm{q}}(\mathbf{r},\mathrm{t}) \tag{1}$$

$$\frac{\partial}{\partial t}C_q(\boldsymbol{r},t)=\beta_q(\boldsymbol{r})\sum_{g'}\nu\Sigma_{f,g'}(\boldsymbol{r},t)\phi_{g'}(\boldsymbol{r},t)-\lambda_q C_q(\boldsymbol{r},t) \tag{2}$$

In Eqs. (1) and (2), standard notation is used; ψ is the angular neutron flux, ϕ is the scalar neutron flux, and C is the concentration of delayed-neutron precursors. The subscripts g and $g'=1,\cdots,G$ denote the energy groups and $q=1,\cdots,Q$ the families of precursors of delayed neutrons.

The spatial distribution of the neutron population in static conditions is obtained from the combination between Eqs. (1) and (2), the time derivatives being set to zero and a factor $1/k$ added to compensate the fission production. Then, the static neutron flux $\psi_{g,0}(\boldsymbol{r},\mathbf{\Omega})$ satisfies the equation:

$$\left[\mathbf{\Omega}\bullet\nabla+\Sigma_{t,g,0}(\boldsymbol{r})\right]\psi_{g,0}(\boldsymbol{r},\mathbf{\Omega})=$$
$$\int_{4\pi}\sum_{g'}\Sigma_{s,g'\to g,0}(\boldsymbol{r},\mathbf{\Omega}'\to\mathbf{\Omega})\psi_{g',0}(\boldsymbol{r},\mathbf{\Omega}')d\mathbf{\Omega}'$$
$$+\frac{1}{k}\left[\frac{\chi_{p,q}(\boldsymbol{r})}{4\pi}\left(1-\sum_q\beta_q(\boldsymbol{r})\right)+\frac{1}{4\pi}\sum_q\chi_{d,q,g}(\boldsymbol{r})\beta_q(\boldsymbol{r})\right]\sum_{g'}\nu\Sigma_{f,g',0}(\boldsymbol{r})\phi_{g',0}(\boldsymbol{r}) \tag{3}$$

Equation (3) corresponds to an eigenvalue problem, whose largest eigenvalue has the physical meaning of the effective multiplication factor k_{eff}.

In reactor neutron noise problems, the source of perturbation may be described as small fluctuations of the macroscopic neutron cross sections of the system under stationary conditions, which in turn induce small fluctuations in the neutron flux. The reactor neutron noise can be obtained from the difference between the neutron flux calculated with Eqs. (1)–(2) and the static neutron flux calculated with Eq. (3).

Solving the reactor neutron noise equations in the time domain is computationally expensive. A more convenient approach is to treat these equations in the frequency (Fourier) domain because it requires to run simulations only for the specific frequencies associated with the noise source. The frequency-domain reactor neutron noise equation can be derived as follows. The neutron flux, the concentration of precursors, and the nuclear cross sections in Eqs. (1)–(2) are modelled as the sum of a static mean value and a small, stationary fluctuating part. The other system parameters, including the effective multiplication factor k_{eff}, are assumed to be constant with respect to time. Equation (3) is subtracted from Eqs. (1)–(2), the second-order perturbation terms are neglected (the so-called "orthodox linearization", see (Pázsit, 1984)), and a Fourier transform is performed on the time variable. The resulting equation reads as:

$$\left[\mathbf{\Omega}\bullet\nabla+\Sigma_{t,g,0}(\boldsymbol{r})+\frac{i\omega}{v_g}\right]\delta\psi_g(\boldsymbol{r},\mathbf{\Omega},\omega)=$$
$$\int_{4\pi}\sum_{g'}\Sigma_{s,g'\to g,0}(\boldsymbol{r},\mathbf{\Omega}'\to\mathbf{\Omega})\delta\psi_{g'}(\boldsymbol{r},\mathbf{\Omega}',\omega)d\mathbf{\Omega}'$$
$$+\frac{1}{\mathrm{k}_{eff}}\left[\frac{\chi_{\mathrm{p,q}}(\mathbf{r})}{4\pi}\left(1-\sum_{\mathrm{q}}\beta_{\mathrm{q}}(\mathbf{r})\right)+\frac{1}{4\pi}\sum_{\mathrm{q}}\chi_{\mathrm{d,q,g}}(\mathbf{r})\frac{\lambda_{\mathrm{q}}\beta_{\mathrm{q}}(\mathbf{r})}{i\omega+\lambda_{\mathrm{q}}}\right]$$
$$\times\sum_{\mathrm{g}'}\nu\Sigma_{\mathrm{f,g}',0}(\mathbf{r})\delta\phi_{\mathrm{g}'}(\mathbf{r},\omega)+S_g(\boldsymbol{r},\mathbf{\Omega},\omega) \tag{4}$$

Equation (4) is a fixed-source problem whose solution yields the induced angular neutron noise $\delta\psi_g$ (and thus also the induced scalar neutron noise $\delta\phi_g$), which is a complex quantity. The parameter ω is the angular frequency of the perturbation and i is the imaginary unit. The term $S_g(\boldsymbol{r},\mathbf{\Omega},\omega)$ in Eq. (4) is the neutron noise source and depends on the perturbation $\delta\Sigma$ of the macroscopic cross sections, i.e.:

$$S_g(\boldsymbol{r},\mathbf{\Omega},\omega)=-\delta\Sigma_{t,g}(\boldsymbol{r},\omega)\psi_{g,0}(\boldsymbol{r},\mathbf{\Omega})$$
$$+\int_{4\pi}\sum_{g'}\delta\Sigma_{s,g'\to g}(\boldsymbol{r},\mathbf{\Omega}'\to\mathbf{\Omega},\omega)\psi_{g',0}(\boldsymbol{r},\mathbf{\Omega}')d\mathbf{\Omega}'$$
$$+\frac{1}{\mathrm{k}_{eff}}\left[\frac{\chi_{\mathrm{p,q}}(\mathbf{r})}{4\pi}\left(1-\sum_{\mathrm{q}}\beta_{\mathrm{q}}(\mathbf{r})\right)+\frac{1}{4\pi}\sum_{\mathrm{q}}\chi_{\mathrm{d,q,g}}(\mathbf{r})\frac{\lambda_{\mathrm{q}}\beta_{\mathrm{q}}(\mathbf{r})}{i\omega+\lambda_{\mathrm{q}}}\right]$$
$$\times\sum_{\mathrm{g}'}\nu\delta\Sigma_{\mathrm{f,g}'}(\mathbf{r})\delta\phi_{\mathrm{g}'}(\mathbf{r},\omega) \tag{5}$$

Equations (4)–(5) are the backbone of the frequency-domain neutron noise solvers implemented in TRIPOLI-4®, APOLLO3®, NOISE-SN and CORE SIM +. On the other hand, the time-dependent solver developed in FEMFFUSION, namely FEMFFUSION-TD, is based on the diffusion approximation of Eqs. (1)–(2). These solvers are briefly described below.

2.1. The stochastic solver in TRIPOLI-4®

A stochastic noise solver in the frequency domain has been implemented in the development version of the Monte Carlo code TRIPOLI-4®

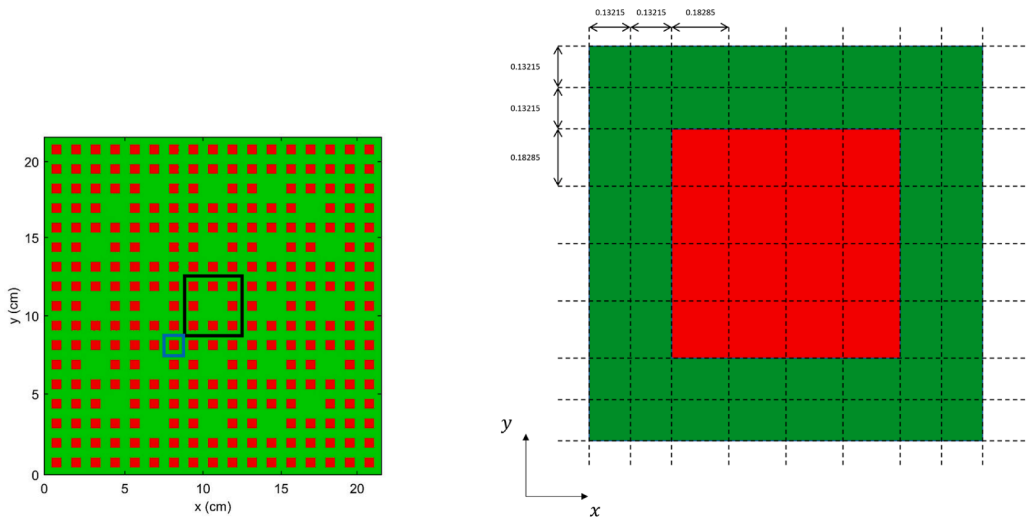

Fig. 1. On the left: simplified UOX fuel assembly with one vibrating fuel pin (blue box) or with a central cluster of 8 vibrating fuel pins (black box); on the right: reference spatial grid for a fuel cell; fuel pins are in red and water region is in green, dimensions are in cm.

(Brun et al., 2015). The continuous-energy version of Eqs. (4)–(5) is solved by transporting particles carrying two statistical weights, one for the real part and one for the imaginary part of the noise field. Particle flights are sampled from an exponential distribution, as for the regular Boltzmann equation, whereas the collision events are modified by the presence of complex operators in the noise equations (an additional imaginary absorption cross section and a complex delayed neutron yield). Such terms are dealt with by correspondingly modifying the particle weights at each collision. A thorough description of the implemented algorithms is available in (Rouchon et al., 2017) and (Rouchon et al., 2019). If required, the noise source term in the continuous-energy version of Eq. (5) is preliminarily computed by running a power iteration (see Eq. (3)) and sampling from the frequency-dependent distributions. Thanks to the continuous-energy treatment of particle transport, the noise solver of TRIPOLI-4® introduces almost no approximations and preserves thus the reference character of the usual Monte Carlo simulations.

2.2. The IDT lattice solver in APOLLO3®

A deterministic noise equation solver in the frequency domain has been implemented in IDT, the lattice solver in APOLLO3® (Schneider et al., 2016) based on the SN discrete ordinates method and on the method of short characteristics (MOSC). The standard iteration loops are applied to the fission source (but the production operator is now complex, as shown in Eq. (4)) and to the scattering source as customary, and an iteration loop between the real and imaginary parts of the reactor neutron noise equation is added, see details in (Rouchon et al., 2020). Thus, the standard one-group transport solver methods can be used, and one can consequently benefit from all numerical methods already implemented in APOLLO3®. At present, the noise solver of IDT can deal with homogeneous Cartesian geometries. If needed, the noise source in Eq. (5) is computed by running a power iteration to solve Eq. (3).

2.3. Noise-SN

The solver NOISE-SN is based on the finite diamond difference method for the spatial discretization, the discrete ordinates method for the angular discretization, and the multi-energy group formalism. The Chebyshev-Legendre quadrature is used to construct the scalar neutron flux from the angular neutron flux. The iterative scheme is accelerated using a Coarse Mesh Finite Difference – CMFD technique. Considering a critical nuclear system with a perturbation described as small fluctuations of the macroscopic neutron cross sections, the solver first calculates the neutron flux and the multiplication factor associated with the static problem given by Eq. (3). Then the reactor neutron noise equations are solved in the frequency domain (see Eqs. (4)–(5)), so that the neutron noise is determined according to the prescribed neutron noise source and the estimated static solution. The numerical methods used in NOISE-SN and their implementation are described in (Yi et al., 2021).

2.4. Core SIM+

The reactor neutron noise simulator CORE SIM+ relies on a two-energy group diffusion model with one family of precursors of delayed neutrons. The numerical scheme can make use of uniform or non-uniform meshes for the spatial discretization of the neutron balance equations. The neutron noise source is modelled as small fluctuations of macroscopic neutron cross sections in a critical nuclear system, and the calculation of the induced neutron noise consists of two steps. In the first step, the static neutron equations (Eq. (3)) are solved via the power iteration method accelerated by Chebyshev polynomials or by a Jacobian Free Newton-Krylov technique. In the second step, the reactor neutron noise equations are solved in the frequency domain (Eqs. (4)–(5)), using the static neutron flux and the multiplication factor previously evaluated and assuming no deviation of the perturbed system from criticality. The numerical solution of the linear systems generated from the power iteration algorithm and from the reactor neutron noise equations is given by the GMRES method combined with an ILU(0) or SGS preconditioner. A comprehensive discussion on the theory, numerical methods, and architecture of CORE SIM+ is available in (Mylonakis et al., 2020) and (Mylonakis et al., 2021).

2.5. Femffusion-TD

FEMFFUSION is an open-source general time-domain code that solves the multigroup time-dependent neutron diffusion equation developed by Universitat Politècnica de València (UPV). This code uses a spatial discretization based on the continuous Galerkin Finite Element Method (FEM) and it can deal with any type of geometry (rectangular, hexagonal, or unstructured) and any problem dimension (1D, 2D and 3D problems). FEMFFUSION can solve different perturbations of the reactor steady state, e.g., rod ejection events. Also, it is possible to solve generic changes in the reactor inserted as a custom set of time-domain cross-sections. Recently, it was updated to simulate in the time domain and in

Table 1
Nuclear data for the fuel assembly, group 1 is for the fast neutrons and group 2 is for the thermal neutrons.

Data	Symbol	Homogeneous square fuel pin	Homogeneous water hole and water blade
Total cross section, group 1 (cm^{-1})	Σ_{t1}	0.3779	0.25411
Total cross section, group 2 (cm^{-1})	Σ_{t2}	0.55064	1.2182
Absorption cross section, group 1 (cm^{-1})	Σ_{a1}	0.025755	0.00079457
Absorption cross section, group 2 (cm^{-1})	Σ_{a2}	0.15788	0.029316
Fission cross section, group 1 (cm^{-1})	Σ_{f1}	0.0057671	0.0
Fission cross section, group 2 (cm^{-1})	Σ_{f2}	0.10622	0.0
Average number of neutrons per fission event	ν	2.59068	0.0
Scattering cross section, group 1 to group 2 (cm^{-1})	Σ_{s12}	0.00086471	0.028124
Velocity, group 1 (cm. s^{-1})	v_1	1.82304E + 07	
Velocity, group 2 (cm. s^{-1})	v_2	4.13067E + 05	
Fraction of delayed neutrons (pcm)	β	535	
Precursor decay time (s^{-1})	λ	0.0851	

the frequency domain the effect of neutron noise perturbations such as generic absorbers of variable strength and mechanically vibrating fuel assemblies. This work includes the results of the time domain module (which is derived from Eqs. (1)–(2)). Neutron noise problems require that the numerical calculations are run using low error tolerances to accurately determine the small fluctuations in the neutron flux. The code is discussed in detail in (Vidal-Ferràndiz et al., 2020a) and is openly available, see (Vidal-Ferràndiz et al., 2020b).

3. Description of the reactor neutron noise benchmark

To verify and compare the noise solvers introduced above, two neutron noise benchmark problems are considered in this work, i.e., the case of the vibration of one fuel pin and the case of the vibration of a central cluster of 8 fuel pins within a 2-dimensional simplified UOX fuel assembly for pressurizer water reactors, see Fig. 1 (on the left). The system specifications are available in (Vinai et al., 2021) and summarized in the following, so that the paper is self-contained. The fuel assembly includes 264 homogeneous square homogeneous fuel pins and 25 homogeneous water holes. The overall size is $21.58cm \times 21.58cm$, the size of the fuel pin is $0.7314cm \times 0.7314cm$, and the size of the water hole is $1.26cm \times 1.26cm$. The fuel assembly is surrounded by a water blade of thickness equal to $0.08cm$.

The reference spatial grid used in the deterministic calculations is such that the fuel pin is divided in cells with size of $0.18285cm \times 0.18285cm$ and the moderator associated with the fuel pin is divided in two identical layers of cells, see Fig. 1 (on the right). The boundary conditions are reflective. The nuclear data are generated with respect to two neutron-energy groups and one family of delayed neutron precursors, and neutron scattering is assumed to be isotropic. All the solvers, including the neutron noise solver in the Monte Carlo code TRIPOLI-4®, use the same set of macroscopic cross sections and neutron kinetics parameters, see Table 1.

The vibrating fuel pins are assumed to periodically oscillate in the x-direction, with an amplitude of $\pm 0.2cm$ and a frequency of $1Hz$.

4. Modelling of vibration of fuel pins

Vibrations of fuel pins in the simplified assembly induce perturbations of the macroscopic cross sections, which are needed to solve the time-dependent Eqs. (1)–(2) or to construct the source term defined by Eq. (5) and used in the frequency-domain Eq. (4).

To illustrate the modelling of this type of perturbation used in the current work, a one-dimensional system is considered along the x-direction and consists of two homogeneous regions separated by an interface whose position at rest is x_0. The vibration of a region with respect to the other one is assumed to be such that the interface oscillates around x_0 according to a time-dependent sinusoidal function with frequency ω_0 and amplitude ε, i.e., the displacement $\varepsilon(t)$ of the interface from x_0 is given by $\varepsilon(t) = \varepsilon \sin(\omega_0 t)$. Then the values of the macroscopic cross sections change consistently with the movement of the interface within the spatial interval between $x_0 - \varepsilon$ and $x_0 + \varepsilon$.

Although the discussion is focused on one vibrating interface, the effect of additional vibrating interfaces can be modelled in the same manner, by linear superposition. The approach can be straightforwardly extended to reactor noise simulations with homogenized nuclear fuel assemblies, allowing a faithful representation of the local nature of mechanical vibrations. In the context of commercial core simulators, an alternative strategy is given in (Chionis et al., 2020) and (Verma et al., 2021), where sets of macroscopic cross sections are generated with respect to the variation of the water-gap associated with the vibrating fuel assembly and used to construct a homogenized noise source, which is however defined over regions larger than the actual location of the perturbation.

The following summarizes the exact treatment in the Fourier space used for the Monte Carlo calculations, the ε/d approximation used for the deterministic calculations in the frequency domain, and the approach used for the time-dependent calculations.

4.1. Exact model

An exact model that describes the variations of macroscopic cross sections induced by a periodic vibration of an interface is discussed in (Rouchon and Sanchez, 2015) and (Zoia et al., 2021), and it is the basis for the Monte Carlo sampling method of the neutron noise source implemented in TRIPOLI-4®. Accordingly, the perturbation of the generic macroscopic cross section Σ_α at position x can be written as:

$$\delta\Sigma_\alpha(x,E,t) = \Delta\Sigma_\alpha(E)(H(x-x_0) - H(x-x_0-\varepsilon\sin(\omega_0 t))) \quad (6)$$

In the equation above, $\Delta\Sigma_\alpha$ is the difference between the macroscopic cross sections associated with the regions on the left and on the right of the interface, respectively, and H is the Heaviside step function.

The perturbation $\delta\Sigma_\alpha(x,E,t)$ may be expanded in a Fourier series whose coefficients are determined using Eq. (6). Then, the Fourier transform is performed with respect to time to obtain the relationships in the frequency domain, i.e.:

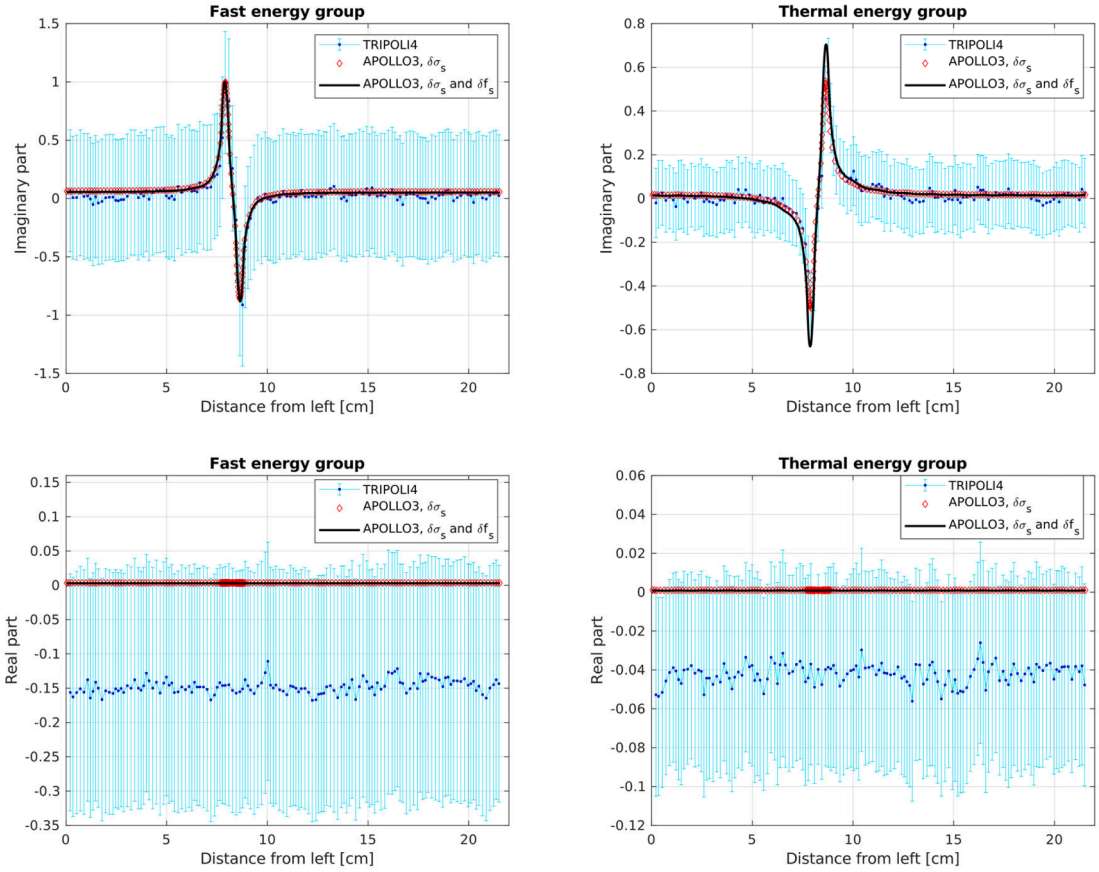

Fig. 2. Vibration of a single vibrating fuel pin; TRIPOLI-4® (blue and cyan), APOLLO3® without perturbed scattering distribution (red), and APOLLO3® with fully perturbed scattering term (black); imaginary part (top) and real part (bottom) of the fast and thermal neutron noise, along the horizontal line crossing the vibrating fuel pin, normalized by the maximum noise amplitude.

$$\delta\Sigma_\alpha(x,E,\omega) = \Delta\Sigma_\alpha(E) \times \begin{cases} c_{\alpha,0}(x,x_0)\delta(\omega) + \sum_{n=1}^{\infty} c_{\alpha,n}(x,x_0)\left(\delta(\omega-n\omega_0) + \delta(\omega+n\omega_0)e^{in\pi}\right), & x_0 < x \le x_0+\varepsilon \\ \left(c_{\alpha,0}(x,x_0)-2\pi\right)\delta(\omega) + \sum_{n=1}^{\infty} c_{\alpha,n}(x,x_0)\left(\delta(\omega-n\omega_0) + \delta(\omega+n\omega_0)e^{in\pi}\right), & x_0-\varepsilon \le x < x_0 \\ 0, \text{ otherwise} \end{cases} \tag{7}$$

In Eq. (7), $\delta(\omega)$ and $\delta(\omega \pm n\omega_0)$ are delta functions, and the Fourier coefficients are equal to:

$$\begin{aligned} c_{\alpha,0}(x,x_0) &= \pi - 2\arcsin\left(\frac{x-x_0}{\varepsilon}\right) \\ c_{\alpha,n}(x,x_0) &= 2\frac{\sin(n\arccos((x-x_0)/\varepsilon))}{n}e^{-in\pi/2},\ n \ge 1 \end{aligned} \tag{8}$$

4.2. The ε/d method

For the deterministic calculations in the frequency domain, the so-called ε/d method is applied (Pázsit, 1977). In the derivation, the Heaviside step function in Eq. (6) is expanded about $(x - x_0)$ as a Taylor series truncated at the first order and the Fourier transform is performed with respect to time. This allows expressing the perturbation of the generic macroscopic cross section Σ_α as:

$$\delta\Sigma_\alpha(x,E,\omega) = \Delta\Sigma_\alpha(E)(-i\pi\varepsilon)\delta(x-x_0)\delta(\omega-\omega_0) \tag{9}$$

As discussed in (Zoia et al., 2021), the spatial delta function in Eq. (9) may be approximated as $\delta(x-x_0) \cong 1/2\varepsilon$ for $x \in [x_0-\varepsilon, x_0+\varepsilon]$, so that the model reads:

$$\delta\Sigma_\alpha(x,E,\omega) = \begin{cases} -i\frac{\pi}{2}\Delta\Sigma_\alpha(E)\delta(\omega-\omega_0), & \text{with } x_0-\varepsilon \le x \le x_0+\varepsilon \\ 0, \text{ otherwise} \end{cases} \tag{10}$$

4.3. Time-dependent model

The FEMFFUSION-TD simulations rely on an alternative approach, see (Vidal-Ferràndiz et al., 2020a). Given a fixed spatial grid and a fixed

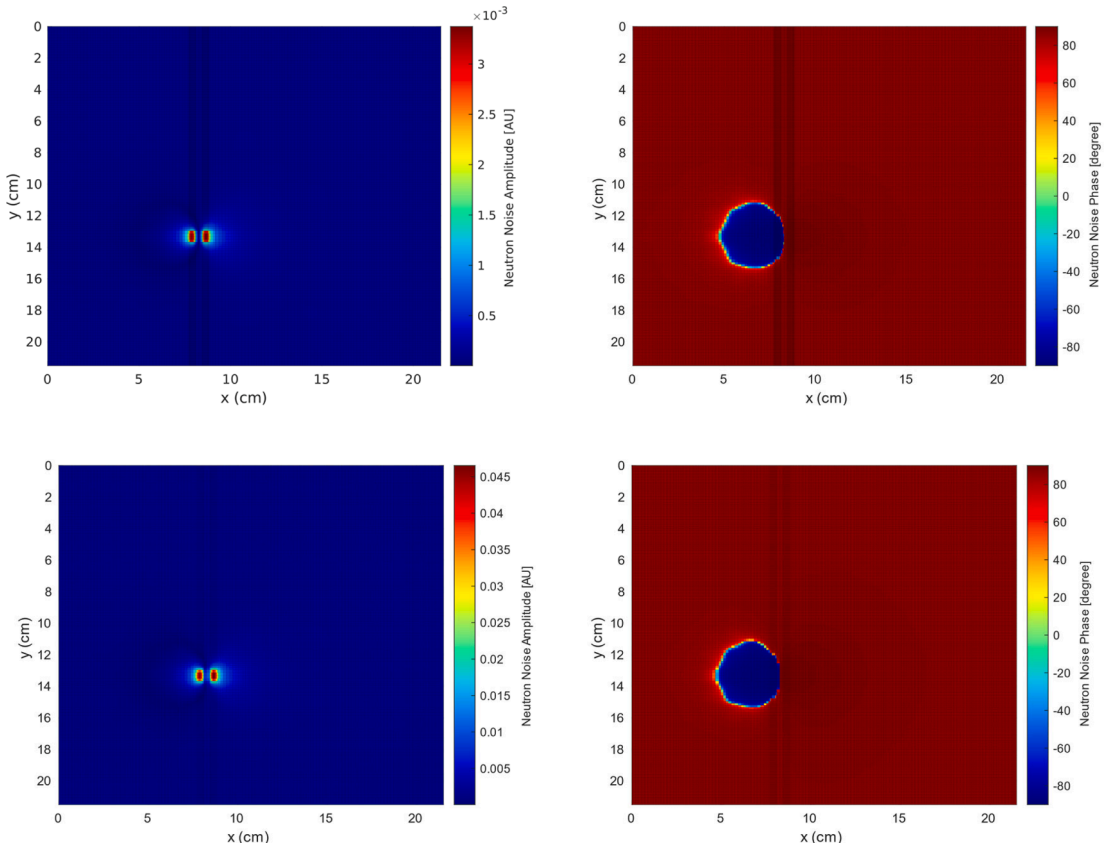

Fig. 3. Case of one single vibrating fuel pin; comparison between APOLLO3® (top, with S32) and NOISE-SN (bottom, with S320); thermal noise absolute amplitude (left) and phase (right).

time grid, the macroscopic cross sections associated with the computational cells that are directly affected by the movement of a vibrating interface are changed according to the actual position of the interface at each time step. Then, these macroscopic cross sections are a combination of the macroscopic cross sections of the two regions separated by the interface, weighted by the volumetric fractions of the two regions in the cells.

5. Simulation results

The solvers presented in section 2 are used to simulate the two neutron noise problems defined in section 3. The objectives of the analysis are to compare and verify stochastic and deterministic neutron noise transport solutions, to investigate the impact of the angular discretization on the neutron noise calculated with the discrete ordinates method, and to assess the accuracy of the diffusion approximation via the higher-order results.

The effective multiplication factor and the neutron fluxes in the static configuration of the simplified fuel assembly were calculated with the solvers and compared in a previous work, see (Vinai et al., 2021). The conclusions were that the higher-order solvers agree in terms of both k_{eff} and static neutron flux, while the lower-order solvers (i.e., CORE SIM+ and FEMFFUSION-TD) overestimate k_{eff} (more than 1000 pcm) and underestimate the neutron fluxes (maximum relative difference with respect to TRIPOLI-4® being around -6% in the moderator region).

For the simulations of the two neutron noise problems with deterministic solvers, the reference spatial grid shown in Fig. 1 is refined near the boundaries of the vibrating fuel pins that are perpendicular to the x-direction. The refinement around these boundaries consists of several layers of computational cells with width of the order of $10^{-2}cm$. This is necessary to better reproduce the spatial variation of the neutron flux arising from the small oscillation (whose maximum amplitude is $\pm 0.2cm$) of the fuel pins. Monte Carlo simulations, on the other hand, are mesh-free and thus do not depend on these spatial refinements.

5.1. Stochastic and deterministic neutron transport simulations

As a first verification step, the stochastic and deterministic neutron transport approaches are compared for the case of a single vibrating fuel pin. For this purpose, the frequency-domain neutron noise solvers developed in TRIPOLI-4® and APOLLO3® are used.

When building the neutron noise source for the frequency-domain calculations of the neutron noise induced by the vibration of the fuel pins, all the types of macroscopic neutron cross sections are perturbed around the left and right interface between the moving fuel pin and the moderator region, see Eq. (5) combined with Eqs. (7)–(8) or Eq. (10). The current modelling of the perturbation of the neutron scattering term in TRIPOLI-4®, because of the complexity of the implementation required for the sampling procedure, includes only the fluctuations of the microscopic scattering cross section and neglects the effect on the scattering distribution $f_s(E \to E', \Omega \bullet \Omega')$, which gives the probability of a neutron with energy E and direction Ω to be scattered in dE' about E' and $d\Omega'$ about Ω'. This simplification introduces an approximation in the sampling of the noise source since the scattering distribution is also expected to vary across the material interfaces. Bearing in mind the comparison with TRIPOLI-4®, two different neutron noise sources have been used for the APOLLO3® simulations. The first noise source relies on the perturbation of the scattering term via only the macroscopic scattering cross section, as in TRIPOLI-4®. The second noise source coincides with the definition in Eq. (5) and includes the perturbation of the scattering distribution.

The TRIPOLI-4® and APOLLO3® results, corresponding to the

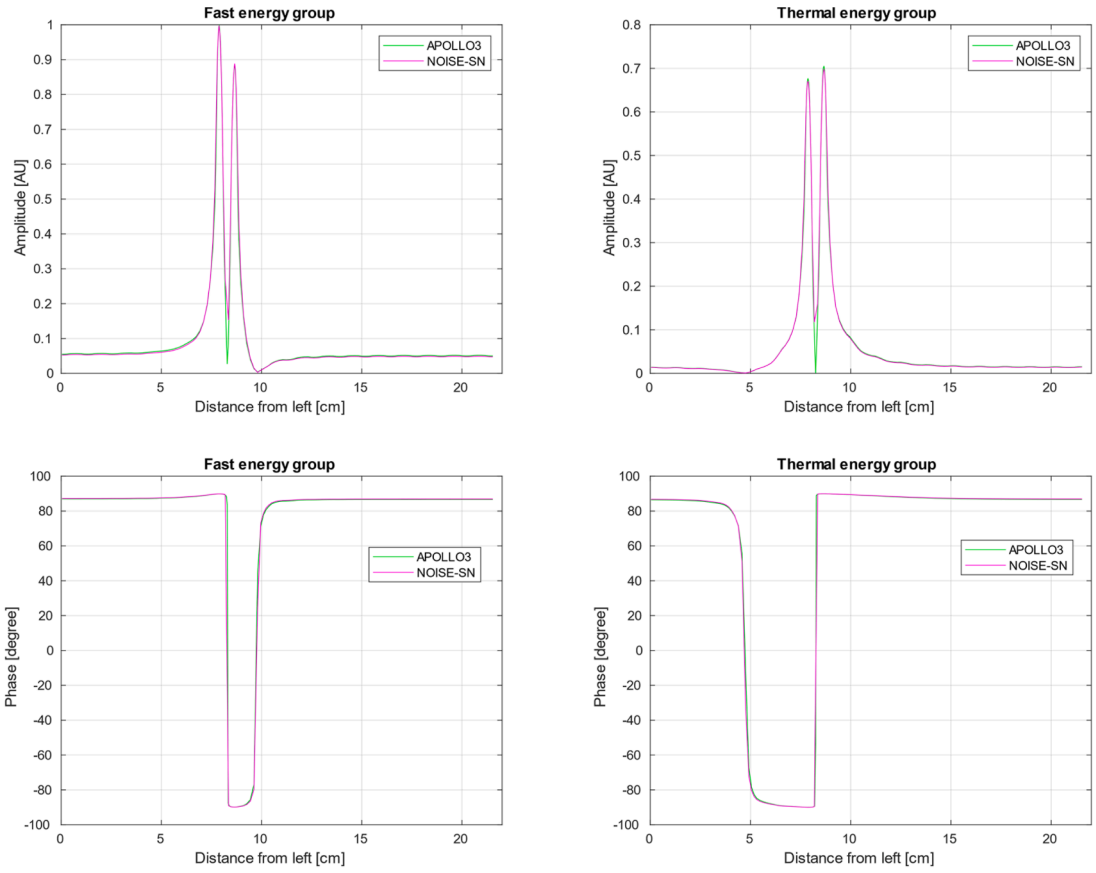

Fig. 4. Case of one single vibrating fuel pin; comparison between APOLLO3® (with S32) and NOISE-SN (with S320) along the horizontal line crossing the vibrating fuel pin; neutron noise amplitude (top, normalized to the maximum value) and phase (bottom) for the fast and thermal energy group.

complex-valued neutron noise field along the horizontal line of the fuel assembly that crosses the vibrating fuel pin, are shown in Fig. 2. For a meaningful comparison, the real and imaginary parts are normalized with respect to the maximum amplitude of the complex neutron noise. The TRIPOLI-4® simulation has been run with 100 inactive cycles with 60′000 neutrons per cycle in order to estimate the noise source using the power iteration, and with a total of 60′000 independent replicas to estimate the neutron noise resulting from the source. For APOLLO3®, the S32 approximation was used with a tolerance criterion for outer iterations of 10^{-6}.

For the imaginary part (top of Fig. 2), TRIPOLI-4® can predict values with good accuracy and its agreement with APOLLO3® (without perturbation of the scattering distribution) is good. On the contrary, the real part of the noise calculated with TRIPOLI-4® has a large statistical error and overall underestimates the one calculated with APOLLO3® (bottom of Fig. 2). This behavior stems from a combination of undersampling and statistical convergence issues in the TRIPOLI-4® simulation, which can be understood as follows. The particles generated from the noise source and transported according to the Monte Carlo procedure carry complex statistical weights: the real and imaginary parts of these weights may be positive and negative, and the fact of adding stochastic contributions with alternating sign in each bin induces an extremely large variance and thus serious problems in statistical convergence. Moreover, the values of the statistical weights may be significantly unbalanced, since the real part of the noise source in the current case is much smaller than the imaginary part (see Eq. (7)–(8), where the main contribution is related to the fundamental frequency ω_0 and is imaginary), and this factor also applies to particles switching from real to imaginary values during the noise transport procedure. The combination of positive and negative weights and the large differences between the real and imaginary parts of the weights further introduces an apparent bias, which is mostly visible in the estimation of the real part of the noise. Future research will investigate the application of a method for weight cancellation that can improve the convergence of the algorithm and provide unbiased solutions with greatly reduced statistical uncertainty (Belanger et al., 2022a). In addition, the APOLLO3® simulations using the two different noise sources (with and without scattering distribution perturbation) are close, which shows that neglecting the perturbation of the scattering distribution does not lead to abnormal behaviors (see lines in red and black in Fig. 2). However, a lower minimum and a higher maximum of the thermal imaginary part are found for the case in which the macroscopic scattering cross section is perturbed via both the microscopic cross section and the scattering distribution.

5.2. *Order of discrete ordinates*

To investigate the impact of the order of discrete ordinates used for the angular discretization, the frequency-domain neutron noise solver available in APOLLO3® with the S32 approximation and the frequency-domain discrete ordinates solver NOISE-SN with the S320 approximation are compared. The spatial computational grids for the two solvers are similar and differ somewhat in the x-direction mesh refinement of the regions over which the left and right physical boundaries of the vibrating fuel pins oscillate and thus the macroscopic cross sections are perturbed. The refinement of each of these regions consists of 10 layers of computational cells of width $0.04cm$ for NOISE-SN, and several layers of computational cells of different width, varying from $0.02cm$ to $0.007cm$, for APOLLO3®. The neutron noise source is modelled using Eqs. (5) and (10) and includes the same, full perturbation of the macroscopic scattering cross sections.

In the noise problem corresponding to the vibration of a single fuel

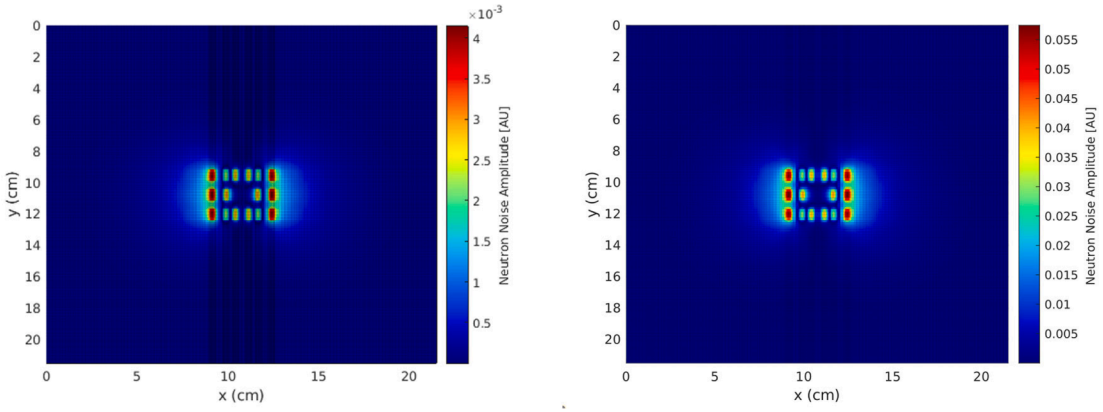

Fig. 5. Case of a central cluster of 8 vibrating fuel pins; thermal neutron noise absolute amplitude obtained from APOLLO3® (left, with S32) and NOISE-SN (right, with S320).

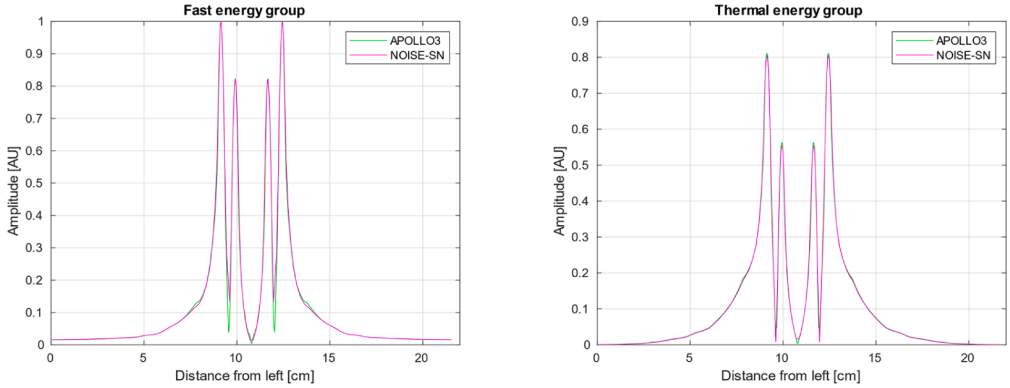

Fig. 6. Case of a central cluster of 8 vibrating fuel pins; fast (left) and thermal (right) neutron noise amplitude (normalized to the maximum value) obtained from APOLLO3® (with S32) and NOISE-SN (with S320), along the mid horizontal crossing the system.

pin, APOLLO3® and NOISE-SN agree well, despite the different order of discrete ordinates, e.g., see the spatial distributions of the thermal neutron noise calculated with the two solvers in Fig. 3 (the two noise amplitudes are in absolute terms and not normalized), and the neutron noise along the horizontal crossing the vibrating fuel pin in Fig. 4 (the noise amplitudes are normalized with respect to the maximum value, which is in the fast group). At the equilibrium points of the left and right boundaries of the vibrating fuel pin, the neutron noise amplitude is maximum. The amplitude of the fast noise is higher than the amplitude of the thermal noise, which is congruous with the fact that the static neutron flux and the neutron noise source are higher in the fast energy group. The spatial distribution of the noise is asymmetric, because of the vicinity of a water hole to the left boundary. The phase has the typical out-of-phase behavior (i.e., a shift of 180°) caused by a mechanical vibration.

In the case of a central cluster of 8 vibrating fuel pins, the angular discretization requires a higher order of discrete ordinates to avoid numerical artifacts, i.e., the so-called ray effect. On the one hand, the S32 approximation (used in APOLLO3®) and the S320 approximation (used in NOISE-SN) calculate close neutron noise amplitudes without any major distortion, e.g., see the spatial distribution of the thermal neutron noise amplitude over the entire fuel assembly in Fig. 5 (where the amplitude is not normalized), and along the mid horizontal of the system that crosses the central cluster of vibrating fuel pins in Fig. 6 (where the amplitude is normalized using the maximum amplitude). On the other hand, the neutron noise phase is particularly sensitive to the issue of ray effect (APOLLO3® and NOISE-SN with the S32 approximation provide similar results, although not shown) and the S320 approximation is needed for an accurate estimation, see Fig. 7. Such an outcome is consistent with previous results obtained from simulations of neutron noise induced by an absorber of variable strength in a mini-reactor core, see (Yi et al., 2021).

5.3. *Assessment of diffusion-based simulations with respect to higher-order solutions*

The time-domain diffusion solver FEMFFUSION-TD and the frequency-domain diffusion solver CORE SIM+ are compared in the case of the vibration of one single fuel pin. The time-dependent reactor neutron noise from FEMFFUSION-TD is processed via a fast Fourier transform to determine the neutron noise amplitude and phase. The differences between the neutron noise calculated with the two diffusion-based solvers are negligible, e.g., see the results along the horizontal in the fuel assembly that crosses the vibrating fuel pin in Fig. 8. As an example of the spatial distribution of the neutron noise in the overall system, the FEMFFUSION-TD results are shown in Fig. 9 (where the noise amplitude is not normalized). Although the static flux and the neutron noise source are higher for the fast energy group, a higher neutron noise absolute amplitude is predicted in the thermal group. This is in contradiction with the results from TRIPOLI-4®, APOLLO3® and NOISE-SN, for which the fast noise absolute amplitude is higher, e.g., see Fig. 4. The neutron noise phase obtained from diffusion and from higher-order simulations are similar, e.g., see the thermal values over the fuel assembly in Figs. 3 and 9.

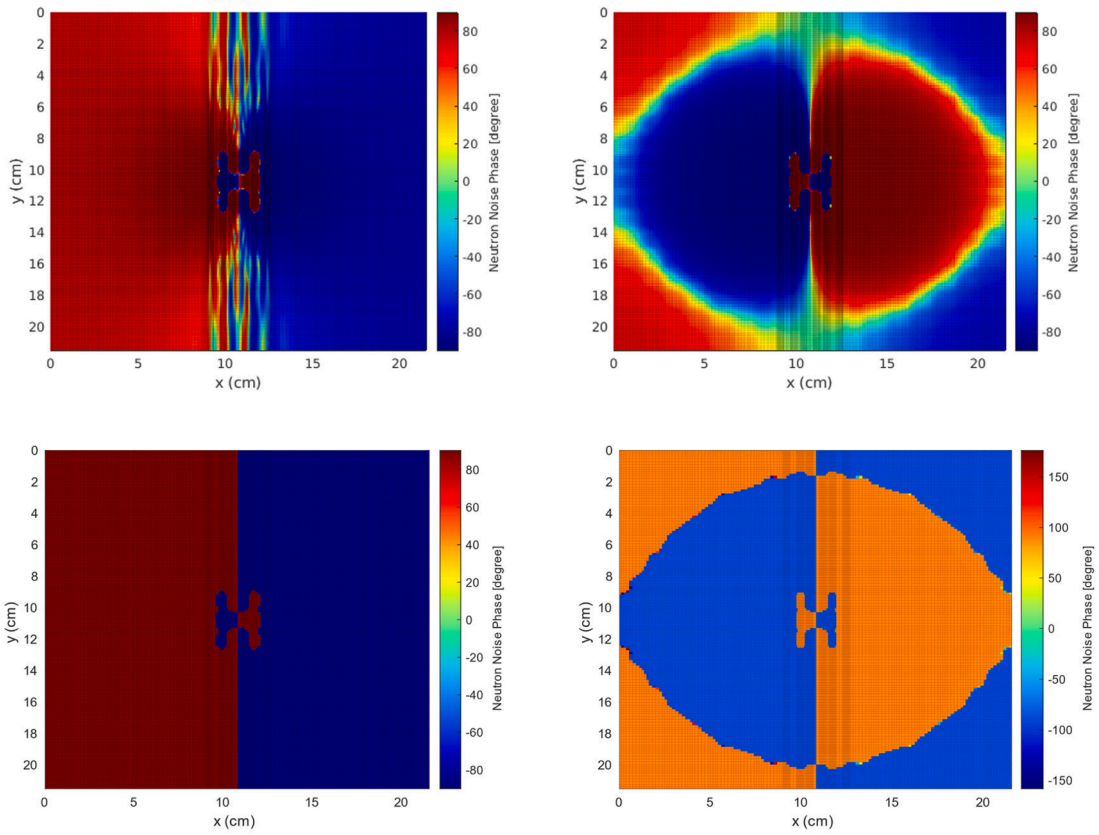

Fig. 7. Case of a central cluster of 8 vibrating fuel pins; comparison between APOLLO3® (top row, with S32) and NOISE-SN (bottom row, with S320); fast (left) and thermal (right) neutron noise phase.

To explain the discrepancy between diffusion and higher-order methods, the noise amplitudes calculated with CORE SIM+ and NOISE-SN along the horizontal that crosses the vibrating fuel pin are analyzed in detail, see Fig. 10 (where the amplitudes are normalized with respect to the Frobenius norm of the static neutron flux). Since linear theory is assumed to be valid, the neutron noise induced by the vibration of the fuel pin is estimated from the combination between two separate simulations, where the perturbation is specified only at the left boundary and only at the right boundary of the vibrating fuel pin, respectively. Such a procedure simplifies the convergence of the solution. In the case of CORE SIM+, the neutron noise obtained from each of the two separate simulations has higher amplitude in the fast group, however the result of the superposition gives a higher amplitude in the thermal group. The neutron noise sources constructed for CORE SIM+ and NOISE-SN are almost identical, so the differences in the calculated neutron noise arises from the specific approximations of the methods. Both solvers calculate the neutron noise as complex quantities in the frequency domain. Close to the location of the noise source, the real part of the neutron noise is relatively small and has a minor impact on the noise amplitude, while the imaginary part of the neutron noise is the dominant contribution and is shown in Fig. 11 (again, the values are normalized with the Frobenius norm of the static neutron flux). If only the perturbation at the left vibrating boundary is taken, the imaginary part at the location of the left vibrating boundary is maximum for the fast group and minimum for the thermal group (see blue lines in Fig. 11). These maxima and minima are less strong in the case of CORE SIM+. Still, at the left boundary and its surroundings, CORE SIM+ and NOISE-SN estimate relatively close imaginary values for the contribution from the perturbation at the right boundary alone (see red lines in Fig. 11). The investigation of the neutron noise around the right boundary leads to a similar outcome. Therefore, the different behavior of the neutron noise stems from the diffusion-based solvers giving inaccurate maxima/minima at the locations of the vibrating boundaries and, in particular, not being able to predict the change of sign of the imaginary part for the thermal neutron noise in the vicinity of the noise source. This may be related to the expected smoothing effect of diffusion in reproducing steep variations of the neutron flux with respect to strong spatial inhomogeneities, such as the local changes in cross sections caused by the vibration of a fuel pin in the moderator.

Differences in value are also found farther from the locations of the perturbation, e.g., NOISE-SN predicts a higher noise amplitude than CORE SIM+ for $x < 5cm$ and for $x > 11cm$ along the horizontal crossing the vibrating fuel pin, see Fig. 10. In these regions of the system, the real part (although it is not shown) is as important as the imaginary part.

Tests have been carried out to investigate different refinements of the spatial computational grid and different amplitudes of the vibration of the fuel pin, and they have led to the same conclusions.

In the case of the central cluster of 8 vibrating pins, FEMFFUSION-TD and CORE SIM+ predict nearly identical neutron noise again. Then, the spatial distribution of the neutron noise calculated with FEMFFUSION-TD is taken as example, see Fig. 12. Two main inconsistencies are found with the results of the APOLLO3® and NOISE-SN transport calculations, i.e., the neutron noise amplitude is higher in the thermal group (as for the problem with one single vibrating fuel pin) and the thermal noise phase has a shift next to the left and right boundaries of the fuel assembly (see the thermal phase in Fig. 3 and Fig. 12).

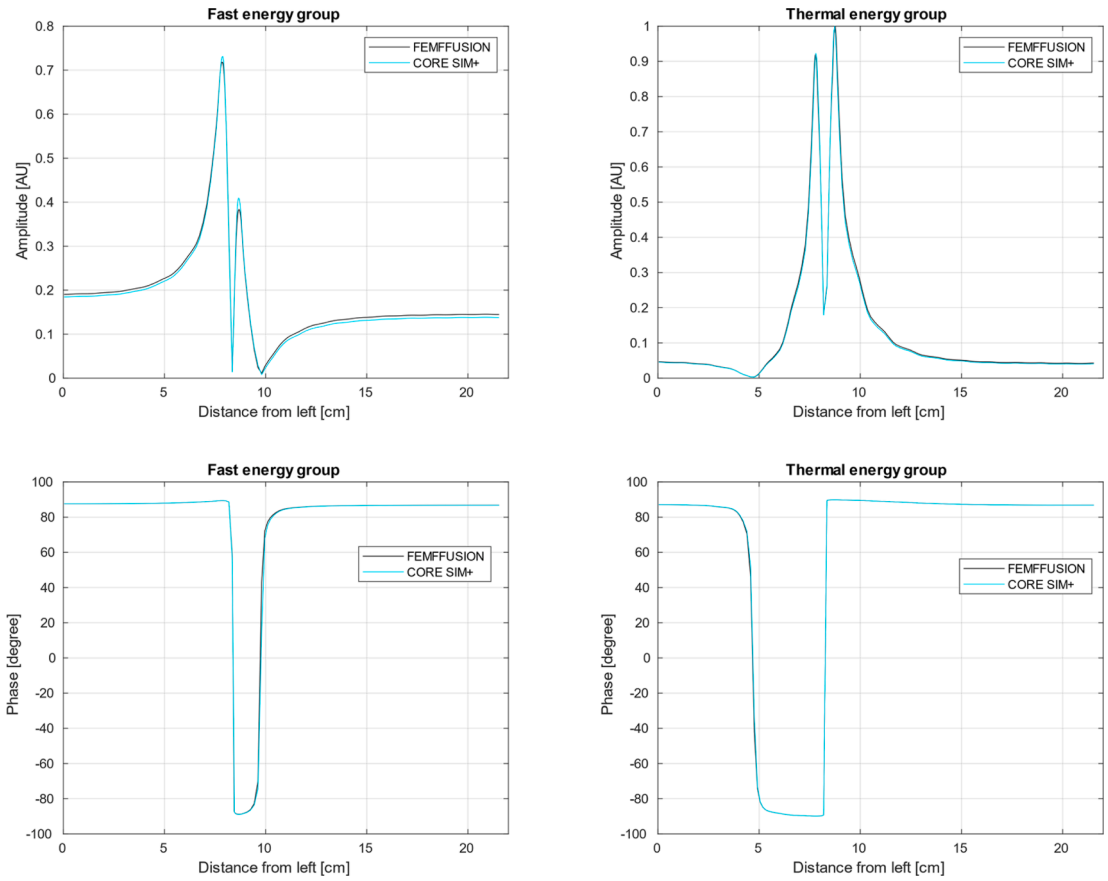

Fig. 8. Case of one single vibrating fuel pin; comparison between FEMFFUSION-TD and CORE SIM+ along the horizontal line crossing the vibrating fuel pin; neutron noise amplitude (top, normalized to the maximum value) and phase (bottom) for the fast and thermal energy group.

6. Conclusions

Several novel reactor neutron noise solvers have been developed in the CORTEX project using different neutron transport methods, such as Monte Carlo, discrete ordinates method, method of characteristics, and diffusion theory. These solvers have been applied to simulate neutron noise induced by mechanical vibrations of one or multiple fuel pins in a 2-dimensional simplified UOX fuel assembly, which are modelled as variations of macroscopic cross sections. Based on the comparisons between their respective results, the performances and issues associated with the different methods have been investigated, leading to three key findings for reactor neutron noise calculations.

First, the stochastic noise solver in TRIPOLI-4® and the deterministic (transport-based) noise solver in APOLLO3® have been compared in the case of one single vibrating fuel pin and predict similar neutron noise fields within the assembly. The effect of including the perturbation of the scattering distribution probability has also been evaluated and has been shown to give slight differences. The real and imaginary parts of the statistical weights in the Monte Carlo calculation result from the sum of positive and negative contributions, and thus they are affected by large statistical uncertainty. Furthermore, because of the unbalance in value between the real and imaginary parts of the noise source associated with the vibration of fuel pins, the real part of the estimated neutron noise has bigger statistical errors and is biased with respect to the deterministic result. Work is then necessary to investigate a more efficient treatment of the complex weights in the Monte Carlo method for these types of neutron noise problems, and it will be discussed in a forthcoming paper specifically devoted to Monte Carlo methods for neutron noise simulations (Belanger et al., 2022b).

Second, in the application of discrete ordinates methods and, in general, of transport-based methods modelling the neutron angular dependence, the balance between the resolution of the angular and spatial discretization is one of the crucial aspects. A too coarse angular grid with respect to the spatial grid may cause ray effect and thus yield an inaccurate solution. In this work, APOLLO3® and NOISE-SN have been used with different orders of discrete ordinates. The comparison has shown that the neutron noise induced by one single vibrating fuel pin over the fuel assembly can be predicted without significant numerical distortion with a relatively low Sn approximation, while the problems involving several vibrating fuel pins require a higher order of discrete ordinates to avoid ray effect and obtain a well-converged solution.

Third, the use of diffusion-based solvers might lead to significant discrepancies in comparison with reference transport-based solvers. Both the calculated static neutron flux and the strength of the neutron noise source are higher in the fast group, as expected. However, the calculated neutron noise amplitude is larger in the thermal group, which is not consistent with the results obtained from the higher-order solvers. According to the analysis carried out in the present work, this may be due to the limitation of diffusion in reproducing variation of the neutron flux with respect to strong spatial inhomogeneities, such as the local changes in cross sections caused by the vibration of a fuel pin in the moderator. For similar reasons, the prediction of the spatial distribution of the neutron noise phase may not be fully accurate in problems with

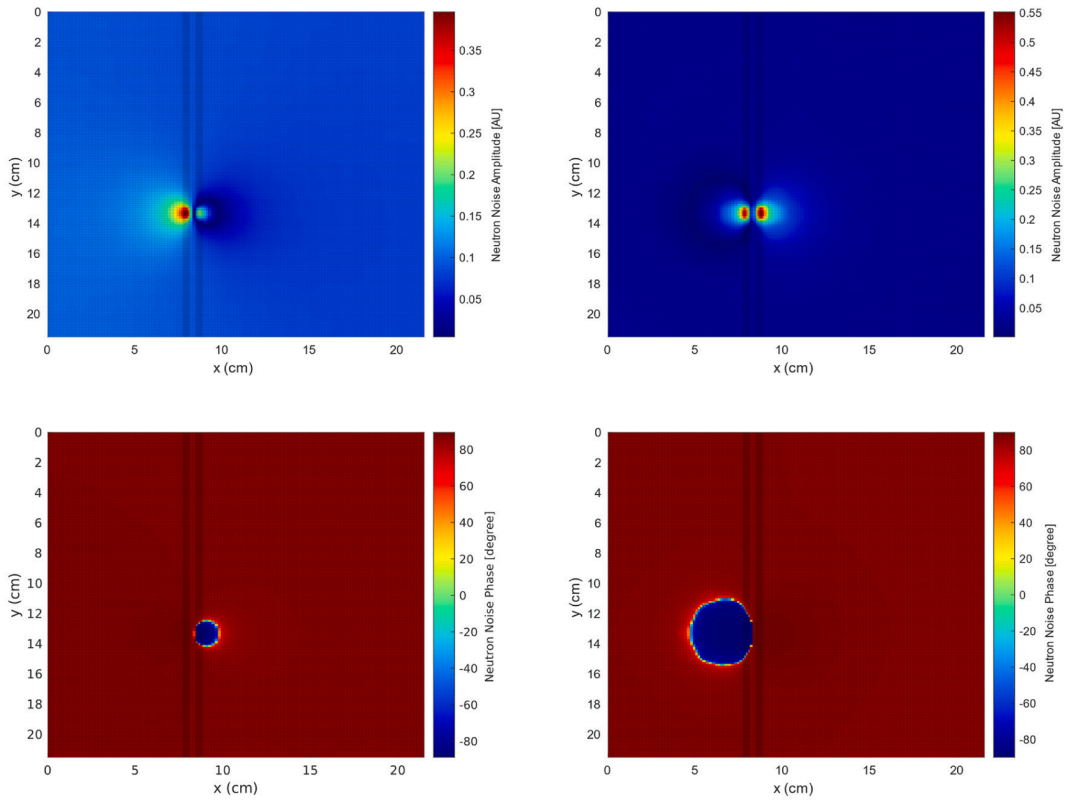

Fig. 9. Case of one single vibrating fuel pin; neutron noise absolute amplitude (top) and phase (bottom) for the fast (left) and thermal (right) energy group calculated with FEMFFUSION-TD.

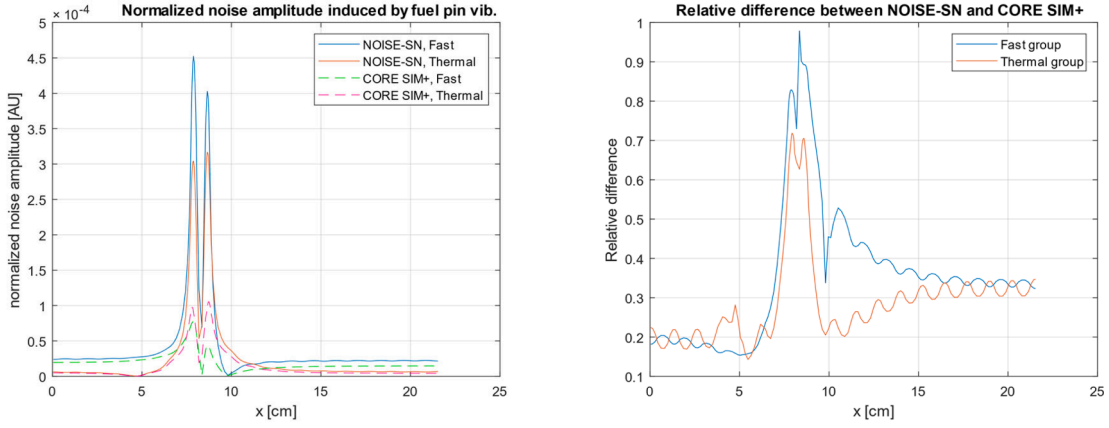

Fig. 10. Case of one single vibrating fuel pin; comparison between NOISE-SN and CORE SIM+ along the horizontal line crossing the vibrating fuel pin; normalized neutron noise amplitude (left) and relative difference between NOISE-SN and CORE SIM+ (right).

clusters of several vibrating fuel pins. Further studies are needed to investigate this issue and its impact on reactor neutron noise simulations for more realistic reactor models, together with possible improvements for the diffusion approximation.

The conclusions thus shed novel light on the use of higher-order transport methods to generate reference solutions for neutron noise problems with mechanical vibrations and on the possible limitations of diffusion-based methods which are commonly applied to simulate reactor neutron noise in nuclear power reactors. These findings contribute to improving the reliability of the new generation of noise solvers currently under development for the purpose of reactor safety.

CRediT authorship contribution statement

P. Vinai: Conceptualization, Formal analysis, Methodology, Software, Writing – original draft, Writing – review & editing. **H. Yi:** Conceptualization, Formal analysis, Methodology, Software, Writing – original draft, Writing – review & editing. **C. Demazière:** Conceptualization, Formal analysis, Methodology, Software, Writing – original draft, Writing – review & editing. **A. Rouchon:** Conceptualization, Formal analysis, Methodology, Software, Writing – original draft, Writing – review & editing. **A. Zoia:** Conceptualization, Formal analysis, Methodology, Software, Writing – original draft, Writing – review & editing. **A. Vidal-Ferràndiz:** Conceptualization, Formal analysis, Methodology, Software, Writing – original draft, Writing – review &

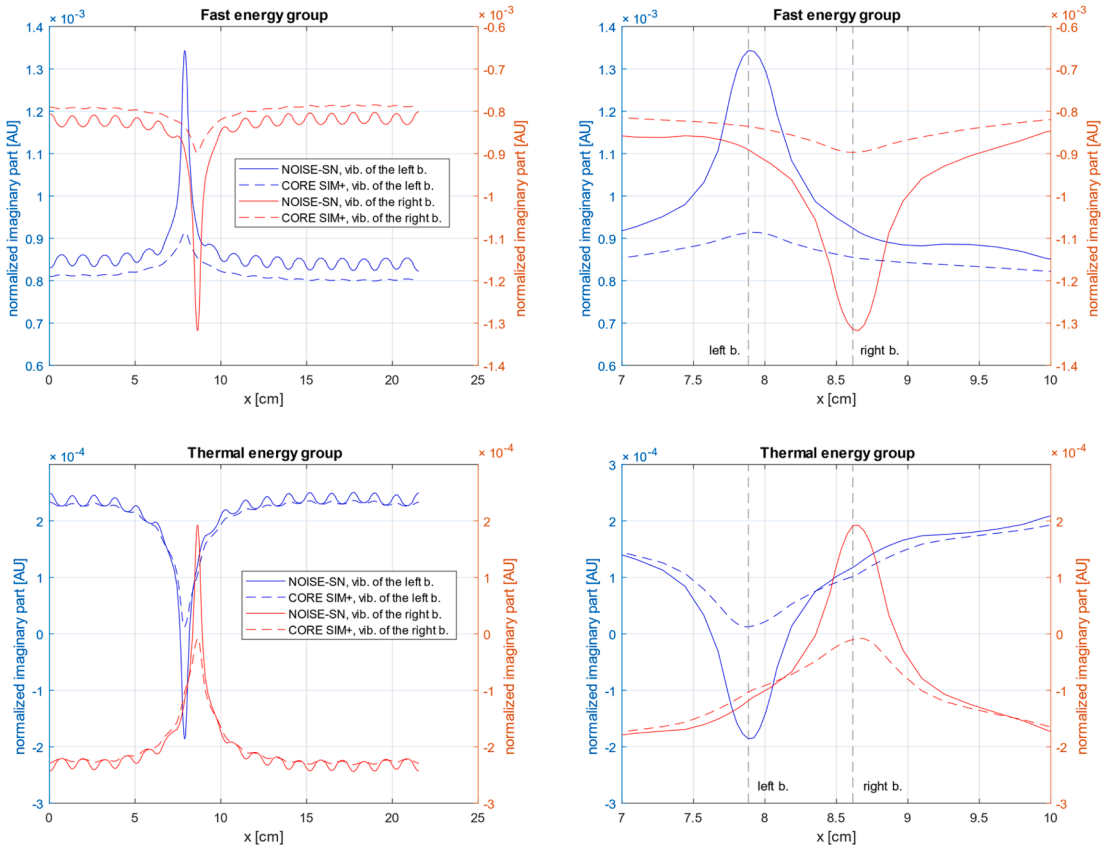

Fig. 11. Case of one single vibrating fuel pin; normalized imaginary part of the neutron noise calculated with NOISE-SN and CORE SIM+ along the horizontal line crossing the vibrating fuel pin; fast energy group (top-left and zoom at top-right) and thermal energy group (bottom-left and zoom at bottom-right).

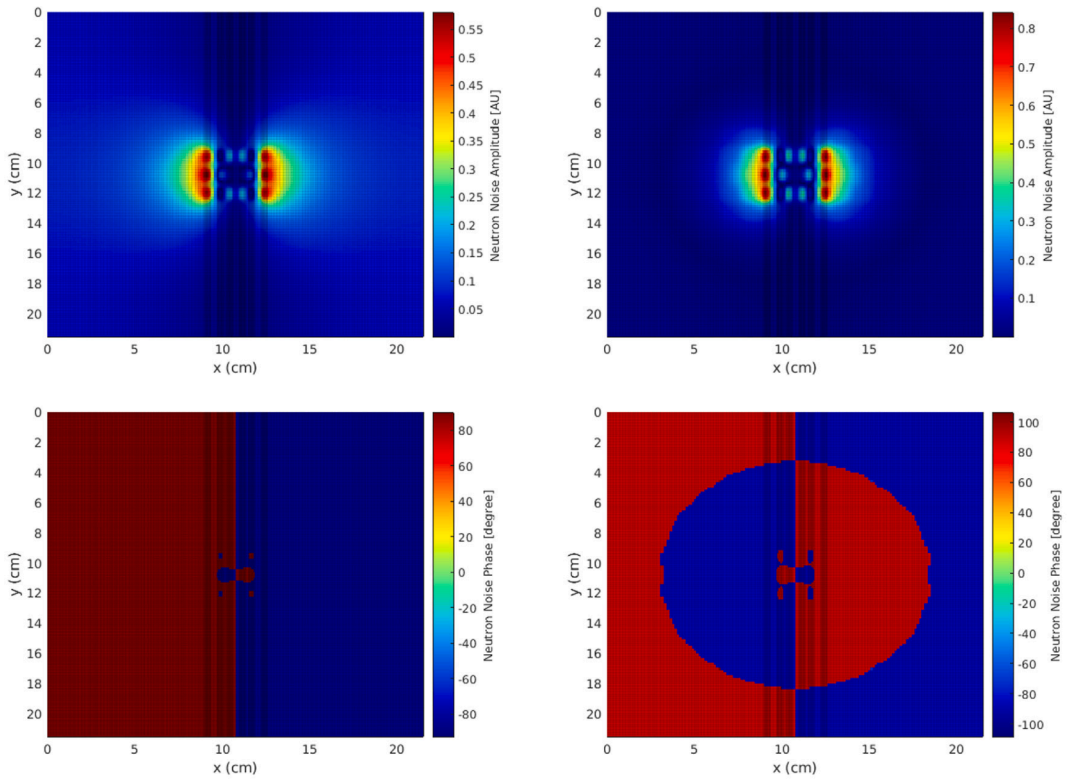

Fig. 12. Case of a central cluster of 8 vibrating fuel pins; neutron noise absolute amplitude (top) and phase (bottom) calculated with FEMFFUSION-TD; fast (left) and thermal (right) energy group.

editing. **A. Carreño:** Conceptualization, Formal analysis, Methodology, Software, Writing – original draft, Writing – review & editing. **D. Ginestar:** Conceptualization, Formal analysis, Methodology, Software, Writing – original draft, Writing – review & editing. **G. Verdú:** Conceptualization, Formal analysis, Methodology, Software, Writing – original draft, Writing – review & editing.

Declaration of Competing Interest

The authors declare that they have no known competing financial interests or personal relationships that could have appeared to influence the work reported in this paper.

Data availability

Data will be made available on request.

Acknowledgments

The research leading to these results received funding from the Euratom Research and Training Program 2014-2018 under grant agreement no. 754316. Part of the computations and data handling was enabled by resources provided by the Swedish National Infrastructure for Computing (SNIC) at C3SE and at UPPMAX, partially funded by the Swedish Research Council through grant agreement no. 2018-05973. TRIPOLI-4® and APOLLO3® are registered trademarks of CEA. A. Rouchon and A. Zoia thank EDF and Framatome for partial financial support.

References

Belanger, H., Mancusi, D., Zoia, A., 2022a. Variance reduction techniques for Monte Carlo neutron noise simulations. In: Proceedings of international conference on physics of reactors – PHYSOR 2022, paper ID: 37344.

Belanger, H., Mancusi, D., Rouchon, A., Zoia, A., 2022b. Variance Reduction and Noise Source Sampling Techniques for Monte Carlo Simulations of Neutron Noise Induced by Mechanical Vibrations. Accepted in Nuclear Science and Engineering.

Brun, E., Damian, F., Diop, C., Dumonteil, E., Hugot, F., Jouanne, C., Lee, Y., Malvagi, F., Mazzolo, A., Petit, O., Trama, J., Visonneau, T., Zoia, A., 2015. TRIPOLI-4®, CEA, EDF and AREVA reference Monte Carlo code. Ann. Nucl. Energy 82, 151–160.

Chionis, D., Dokhane, A., Belblidia, L., Ferroukhi, H., Girardin, G., Pautz, A., 2020. Development and verification of a methodology for neutron noise response to fuel assembly vibrations. Ann. Nucl. Energy 147, 107669.

Demazière, C., Vinai, P., Hursin, M., Kollias, S., Herb, S., 2018. Overview of the CORTEX project. In: In: Proceedings of International Conference on Physics of Reactors – PHYSOR 2018: Reactor Physics Paving the Way Towards More Efficient Systems, pp. 2917–2980.

Mylonakis, A.G., Vinai, P., Demazière, C., 2020. Numerical solution of two-energy-group neutron noise diffusion problems with fine spatial meshes. Ann. Nucl. Energy 140, 107093.

Mylonakis, A., Vinai, P., Demazière, C., 2021. CORE SIM+: a flexible diffusion-based solver for neutron noise simulations. Ann. Nucl. Energy 155, 108149.

Park, J., Lee, J.H., Kim, T.-R., Park, J.-B., Lee, S.K., Koo, I.-S., 2003. Identification of reactor internals' vibration modes of a Korean standard PWR using structural modeling and neutron noise analysis. Prog. Nucl. Energy 43 (1–4), 177–186.

Pázsit, I., 1977. Investigation of the space-dependent noise induced by a vibrating absorber. Atomkernenergie 20, 29–35.

Pázsit, I., 1984. The linearization of vibration-induced noise. Ann. Nucl. Energy 11 (9), 441–454.

Pázsit, I., 1992. Dynamic transfer function calculations for core diagnostics. Ann. Nucl. Energy 19 (5), 303–312.

Rouchon, A., Jarrah, W., Zoia, A., 2019. The new neutron noise solver of the Monte Carlo code TRIPOLI-4®. In: Proceedings of The International Conference on Mathematical and Computational Methods Applied to Nuclear Science and Engineering – M&C 2019, pp. 332-341.

Rouchon, A., Sanchez, R., 2015. Analysis of vibration-induced neutron noise using one-dimension noise diffusion theory. In: Proceedings of International Congress on Advances in Nuclear Power Plants – ICAPP2015, Nice, France, May 3-5, 2015.

Rouchon, A., Zoia, A., Sanchez, R., 2017. A new Monte Carlo method for neutron noise calculations in the frequency domain. Ann. Nucl. Energy 102, 465–475.

Rouchon, A., Le Brun, M.V., Zoia, A., Margulis, M., Blaise, P., 2020. Analysis and comparison of APOLLO3® and TRIPOLI-4® neutron noise solvers. EPJ Web Conf. 247, 21002.

Schneider, D., Dolci, F., Gabriel, F., Palau, J.-M., Guillo, M., Pothet, B., et al., 2016. APOLLO3®: CEA/DEN deterministic multi-purpose code for reactor physics analysis. In: Proceedings of international conference on physics of reactors – PHYSOR 2016, Sun Valley, Idaho, USA.

Tran, H.N., Pázsit, I., Nylén, H., 2015. Investigation of the ex-core noise induced by fuel assembly vibrations in the Ringhals-3 PWR. Ann. Nucl. Energy 80, 434–446.

Verma, V., Chionis, D., Dokhane, A., Ferroukhi, H., 2021. Studies of reactor noise response to vibrations of reactor internals and thermal-hydraulic fluctuations in PWRs. Ann. Nucl. Energy 157, 108212.

Vidal-Ferràndiz, A., Carreño, A., Ginestar, D., Demazière, C., Verdú, G., 2020a. A time and frequency domain analysis of the effect of vibrating fuel assemblies on the neutron noise. Ann. Nucl. Energy 137, 107076.

Vidal-Ferràndiz, A., Carreño, A., Ginestar, D., Verdú, G., 2020b. Repository of FEMFFUSION program: a finite element code for nuclear reactor modelling. https://www.femffusion.imm.upv.es.

Vidal-Ferràndiz, A., Ginestar, D., Carreño, A., Verdú, G., Dokhane, A., Verma, V., Perin, Y., Herb, J., Mylonakis, A., Demazière, C., Vinai, P., 2022. Modelling and simulations of reactor neutron noise induced by mechanical vibrations. Ann. Nucl. Energy 177, 109300.

Vinai, P., Yi, H., Mylonakis, A., Demazière, C., Gasse, B., Rouchon, A., Zoia, A., Vidal-Ferràndiz, A., Ginestar, D., Verdú, G., Yamamoto, T., 2021. Comparison of Neutron Noise Solvers Based on Numerical Benchmarks in a 2-D Simplified UOX Fuel Assembly. In: Proceedings of The International Conference on Mathematics and Computational Methods Applied to Nuclear Science and Engineering – M&C 2021, pp. 2016-2025.

Yamamoto, T., 2013. Monte Carlo method with complex-valued weights for frequency domain analyses of neutron noise. Ann. Nucl. Energy 58, 72–79.

Yamamoto, T., 2018. Implementation of a frequency-domain neutron noise analysis method in a production-level continuous energy Monte Carlo code: verification and application in a BWR. Ann. Nucl. Energy 115, 494–501.

Yi, H., Vinai, P., Demazière, C., 2021. On the simulation of neutron noise using a discrete ordinates method. Ann. Nucl. Energy 164, 108570.

Zoia, A., Rouchon, A., Gasse, B., Demazière, C., Vinai, P., 2021. Analysis of the neutron noise induced by fuel assembly vibrations. Ann. Nucl. Energy 154, 108061.